Supporting Information

Dual-Doping of Sulfur on Mesoporous Carbon as a Cathode for Oxygen Reduction Reaction and Lithium-Sulfur Battery

Dongjun Kim,[†] Geonho Kim,[†] Seoyeah Oh,[†] Jihyeon Park,[†] Seokhee Lee,[†] Seoyoung Yoon,[†] Jiyeon Lee,[†] Wonsik Lee,[†] Tae-Yeol Jeon,[Δ] Eunkyung Cho, [∥] Kwonnam Sohn, [∥] Doo-Kyung Yang, [∥] and Jiwon Kim[*,†,§]*

[†] School of Integrated Technology, College of Engineering, Yonsei University, 85 Songdogwahak-ro, Yeonsu-gu, Incheon, 21983, Republic of Korea.

[§] Integrated Science and Engineering Division, Underwood International College, Yonsei University, 85 Songdogwahak-ro, Yeonsu-gu, Incheon, 21983, Republic of Korea.

[Δ]Beamline Division, Pohang Accelerator Laboratory (PAL), Pohang, 37673, Republic of Korea

[∥] LG Chem., LG Science Park, 30 Magokjungang 10-ro, Gangseo-gu, Seoul, 07796, Republic of Korea.

Corresponding Author

*E-mail: jiwon.kim@yonsei.ac.kr (J.Kim).

Number of pages: 21

Number of Figures: 14

Number of Tables: 6

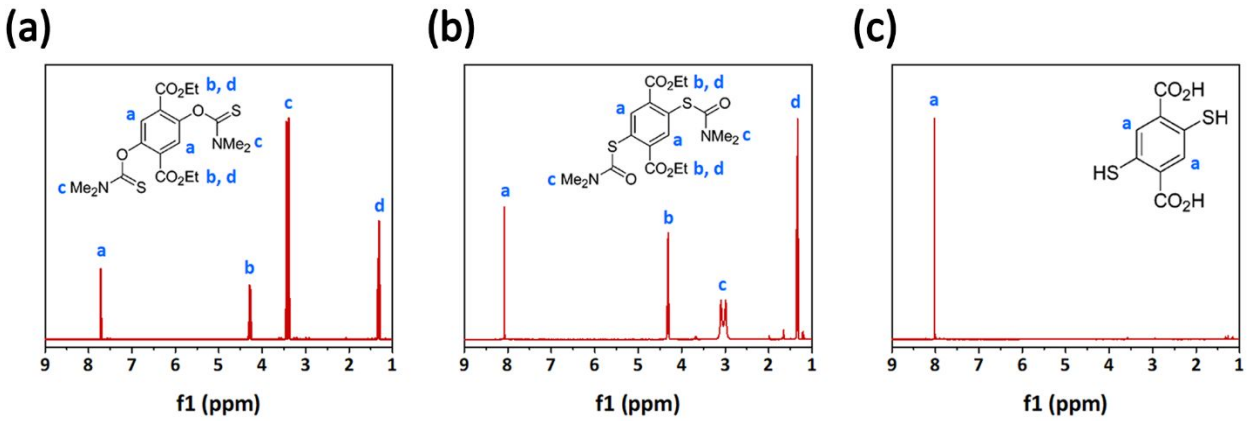

Figure S1. ^{1}H nuclear magnetic resonance (NMR) spectra of (a) diethyl 2,5-bis(dimethylthiocarbamoyloxy)terephthalate, (b) diethyl 2,5-bis(dimethylthiocarbamoylsulfanyl)terephthalate, and (c) 2,5-disulfanylterephthalic acid (BDC-$(SH)_2$).

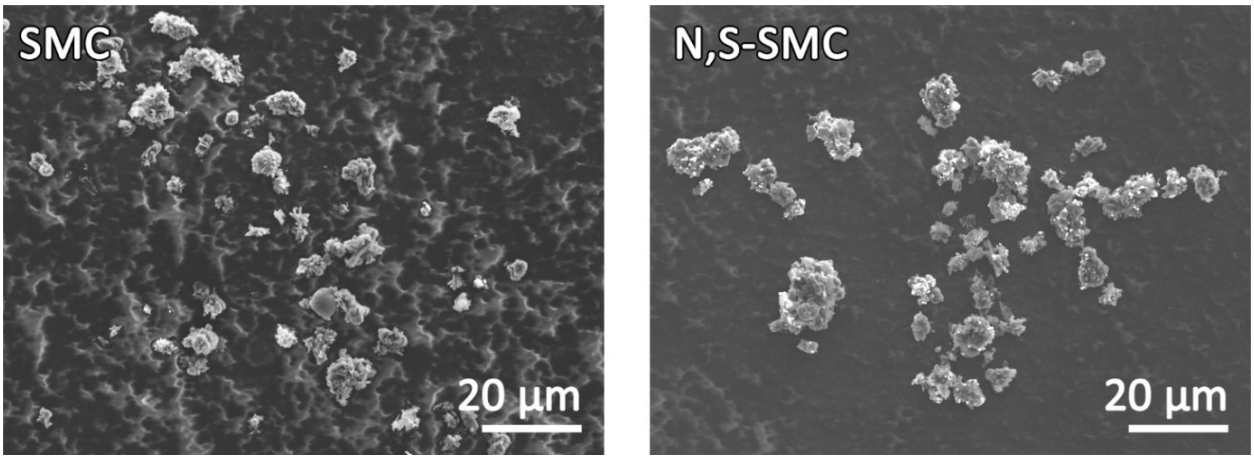

Figure S2. SEM images in low magnification of SMC (left) and N,S-SMC (right)

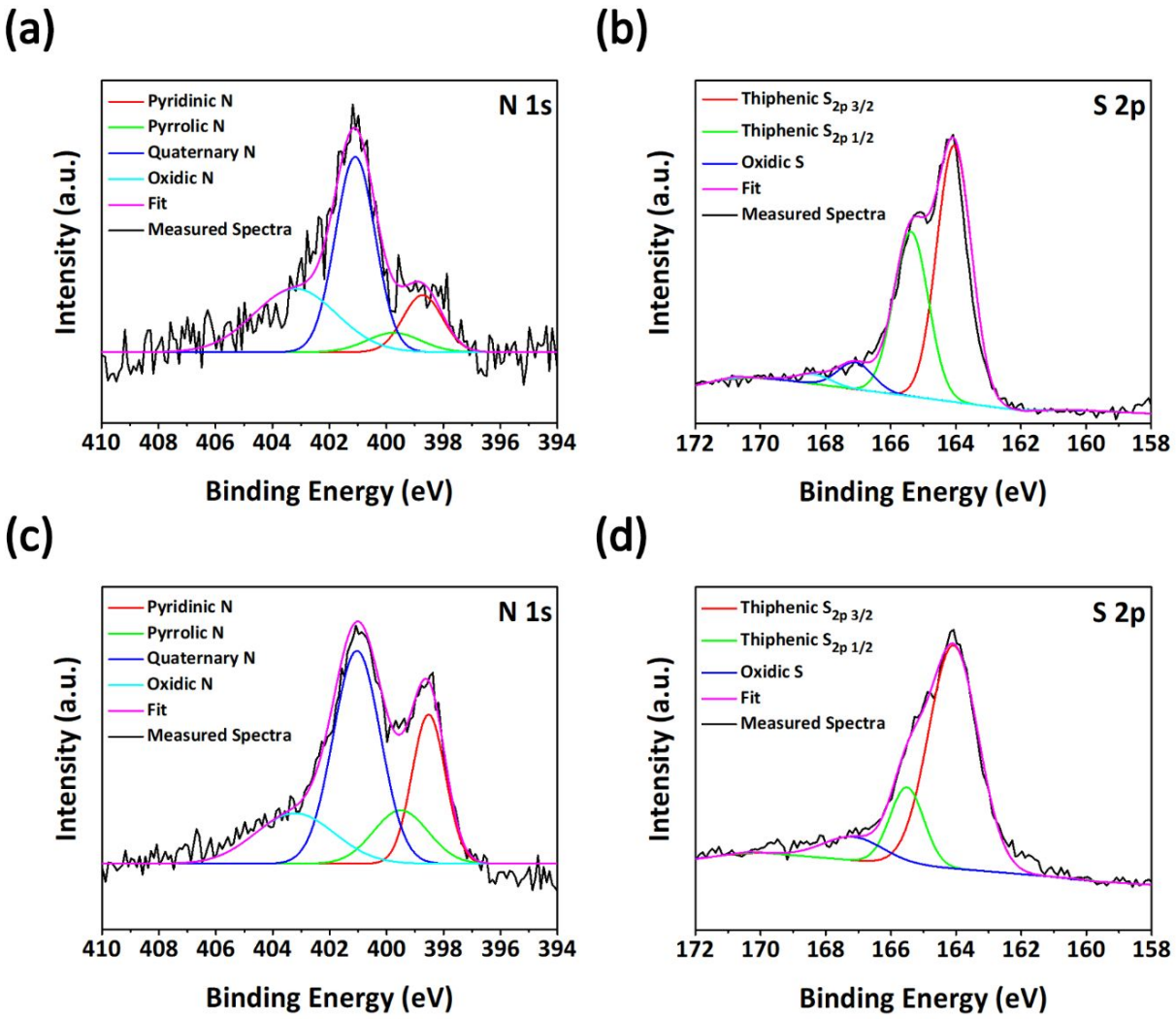

Figure S3. High resolution X-ray photoelectron spectroscopy (HRXPS) spectra of (a) N 1s and (b) S 2p of SMC, (c) N 1s and (d) S 2p of N-SMC.

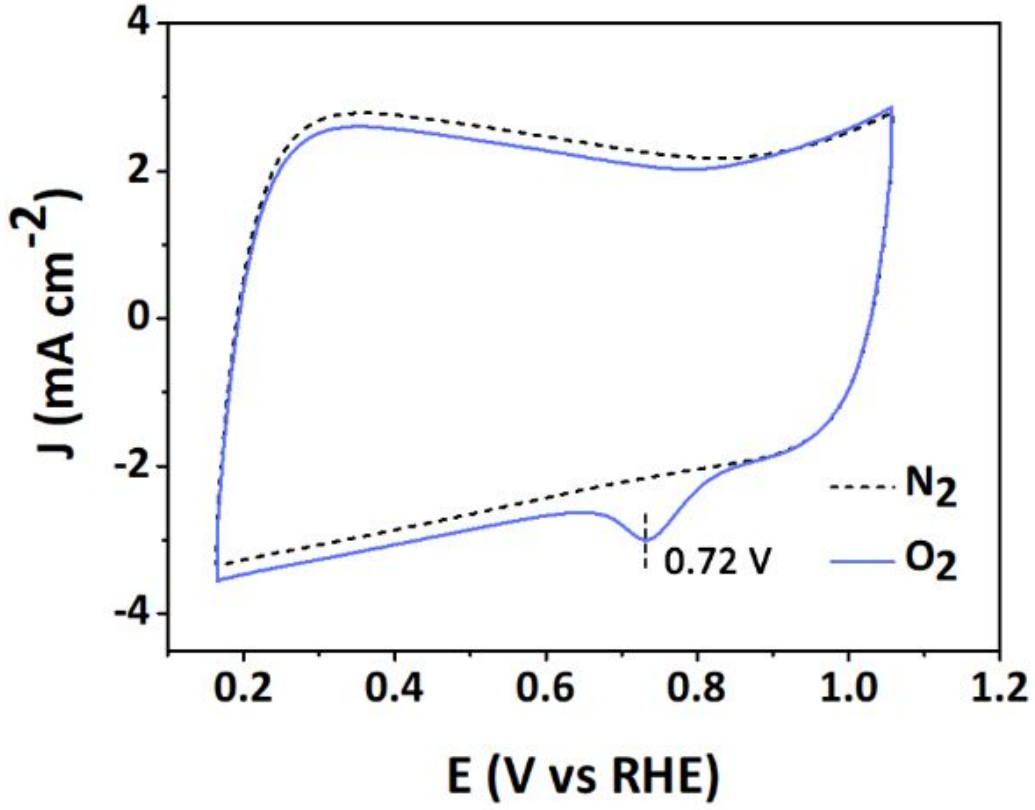

Figure S4. Cyclic voltammetry (CV) of SMC in N_2- and O_2-saturated 0.1 M KOH solution.

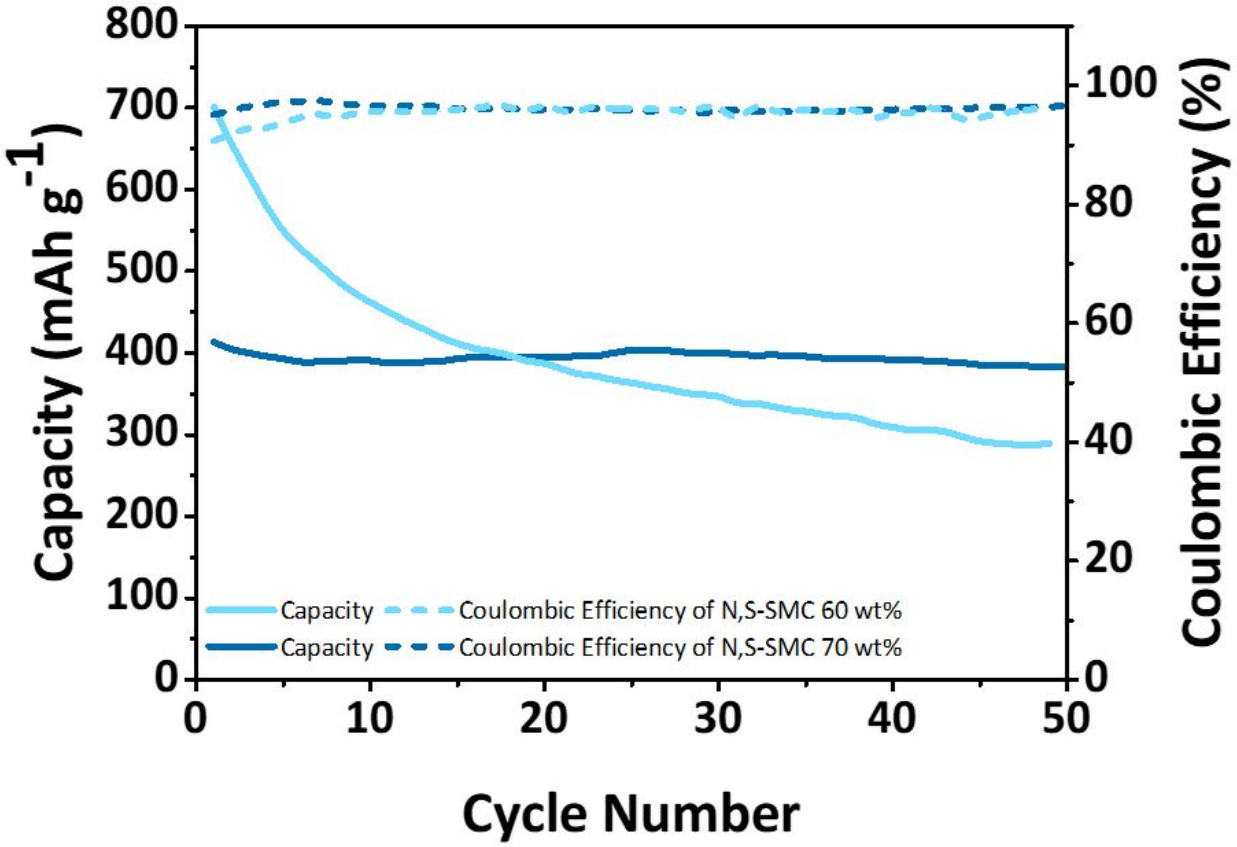

Figure S5. Cyclic performance and Coulombic efficiency of N,S-SMC with sulfur loading of 60 wt% and 70 wt% at the current density of 0.1 C (1 C = 1675 $mA \cdot g^{-1}$) in the voltage range of 1.5-2.8 V versus Li^+/Li.

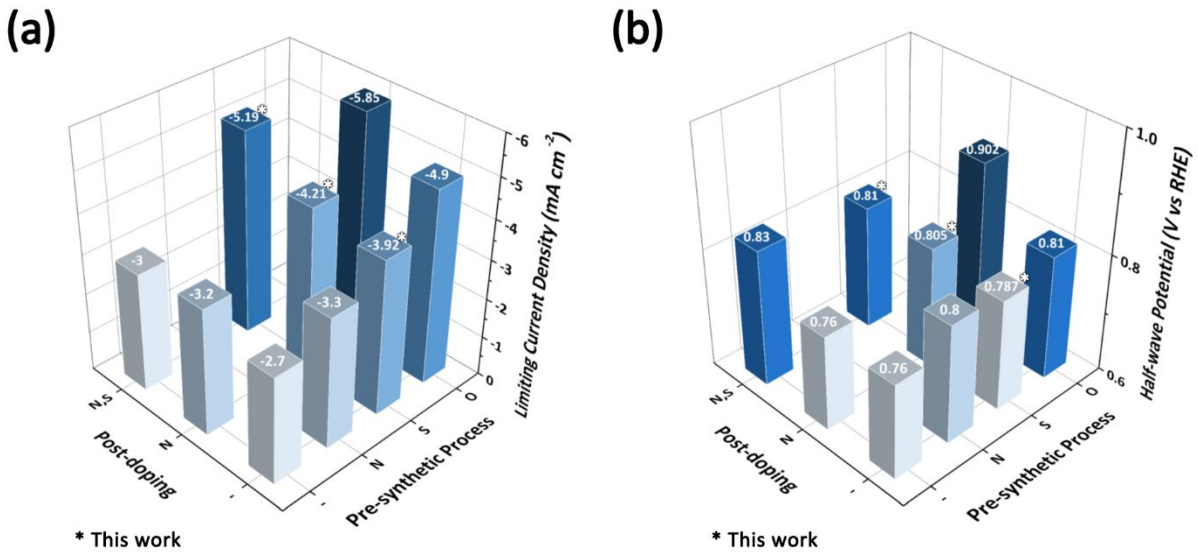

Figure S6. 3D histograms of (a) limiting current density and (b) half-wave potential of pre-synthetic processed and post-doped MOF derived porous carbon employed as catalysts for oxygen reduction reaction (ORR).

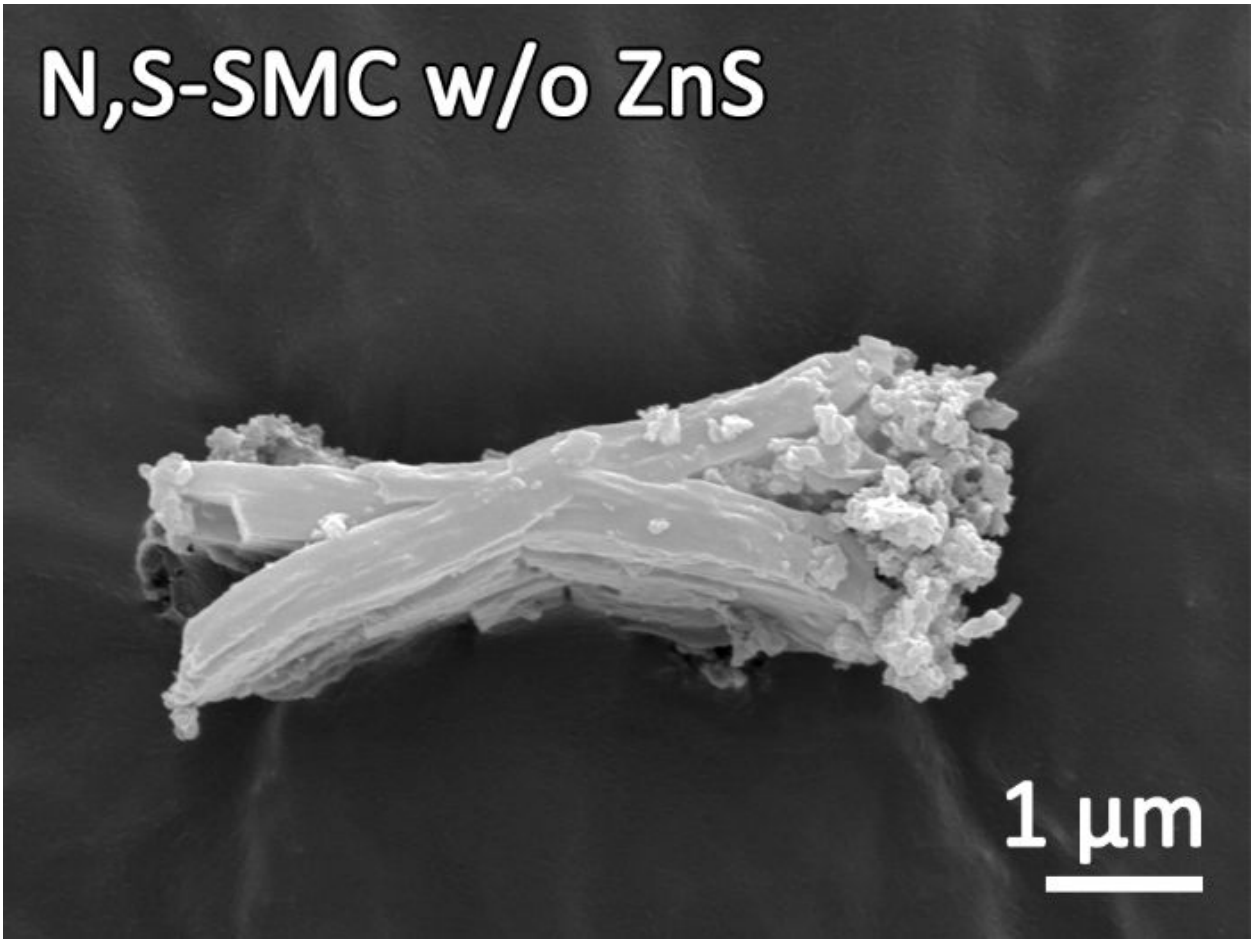

Figure S7. Scanning electron microscopy (SEM) image of N,S-SMC w/o ZnS.

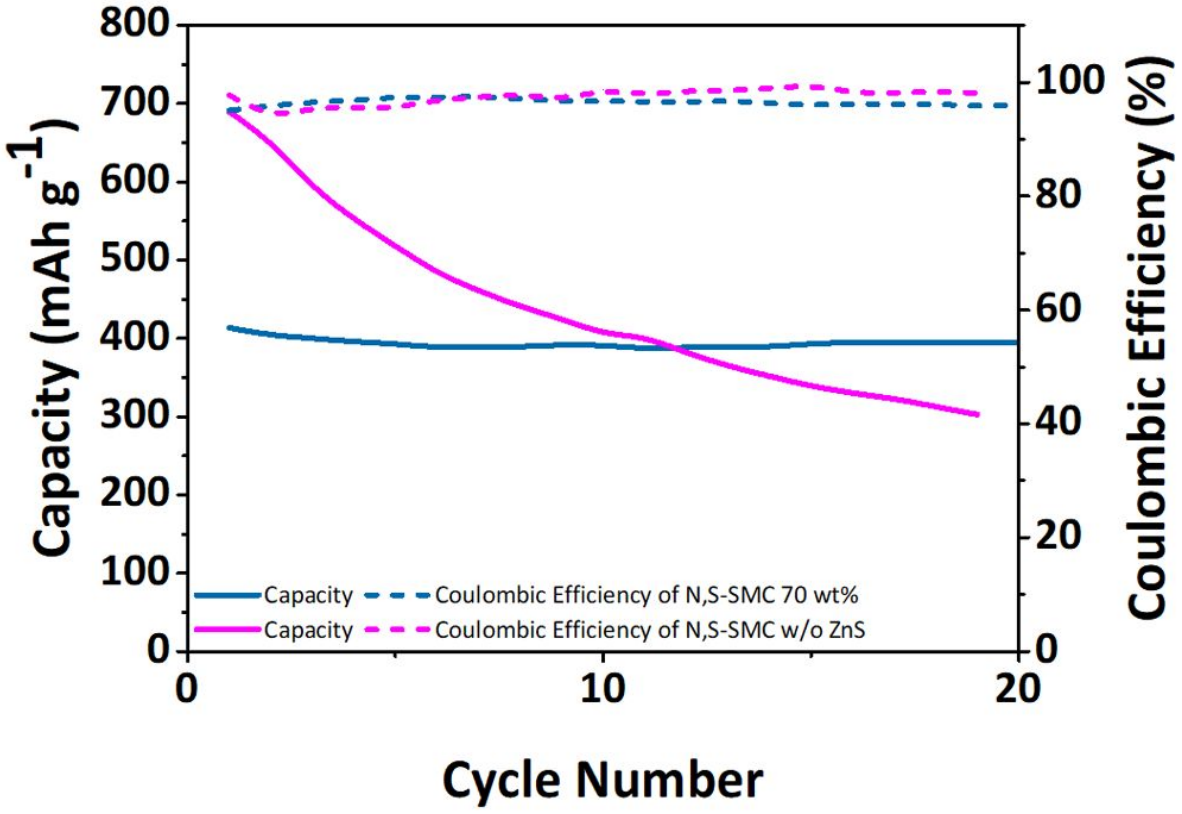

Figure S8. Cyclic performance and Coulombic efficiency of N,S-SMC and N,S-SMC w/o ZnS at the current density of 0.1 C (1 C = 1675 $mA \cdot g^{-1}$) in the voltage range of 1.5-2.8 V versus Li^+/Li.

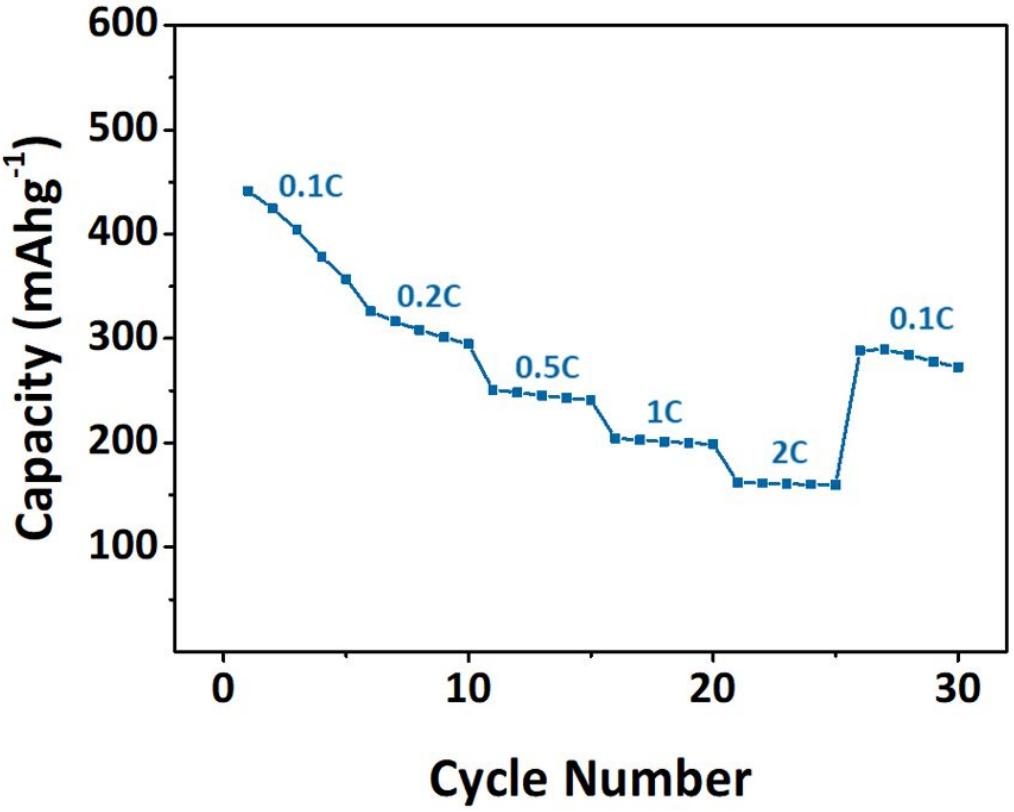

Figure S9. Rate performance of N,S-SMC from 0.1 to 2 C.

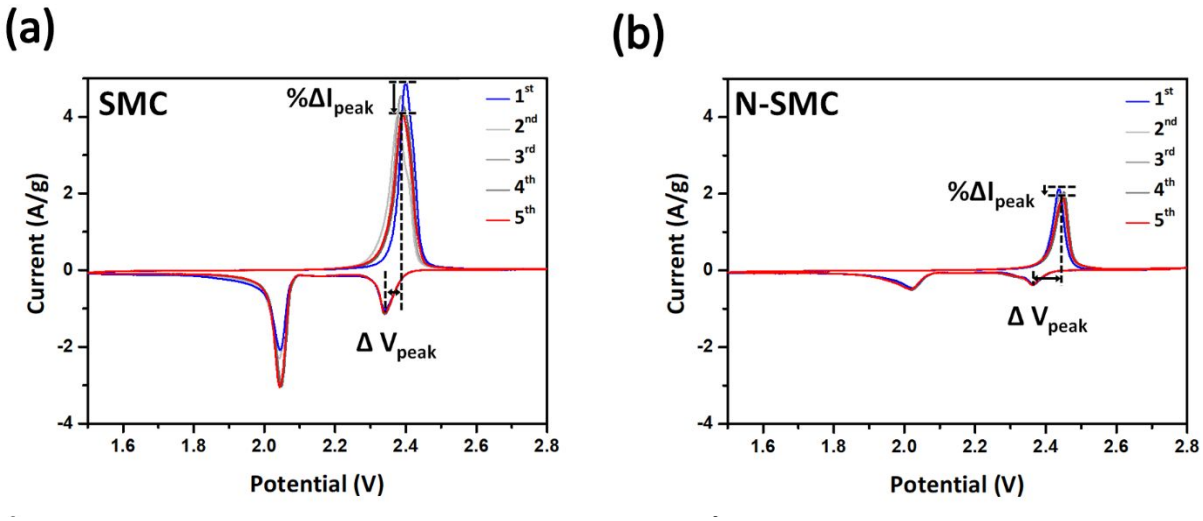

Figure S10. Cyclic voltammetry (CV) curves of (a) SMC and (b) N-SMC at 0.1 $mV \cdot s^{-1}$.

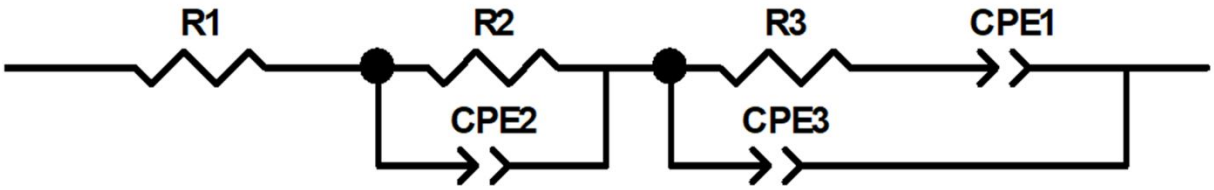

Figure S11. Equivalent circuit corresponding to the Nyquist plot and determined each resistance element (R_1, R_2, R_3).

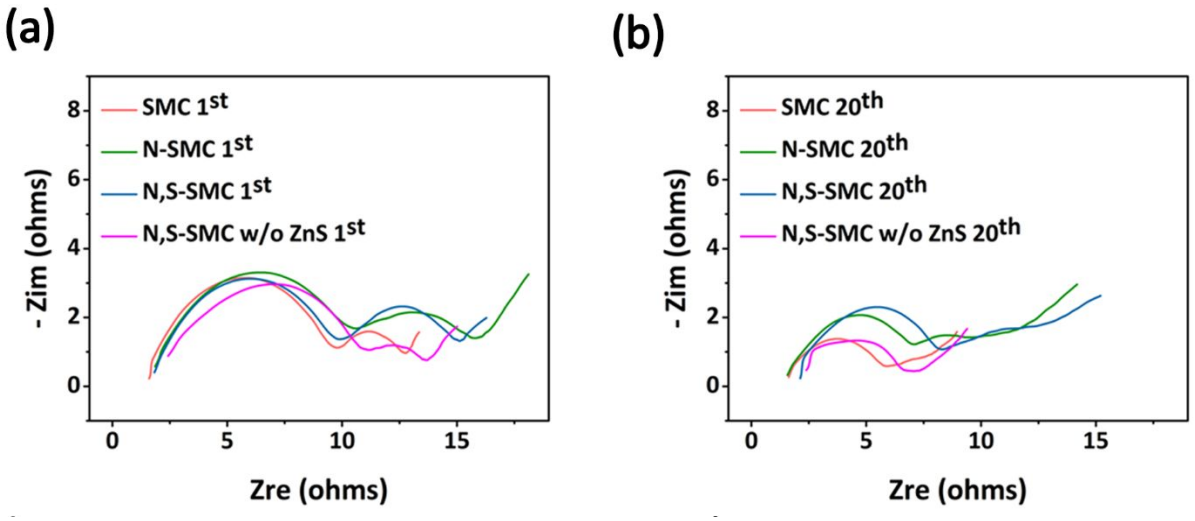

Figure S12. Electrochemical impedance spectroscopy (EIS) results of SMC, N-SMC, N,S-SMC, and N,S-SMC w/o ZnS charged to 2.8 V at (a) 1st and (b) 20th cycles.

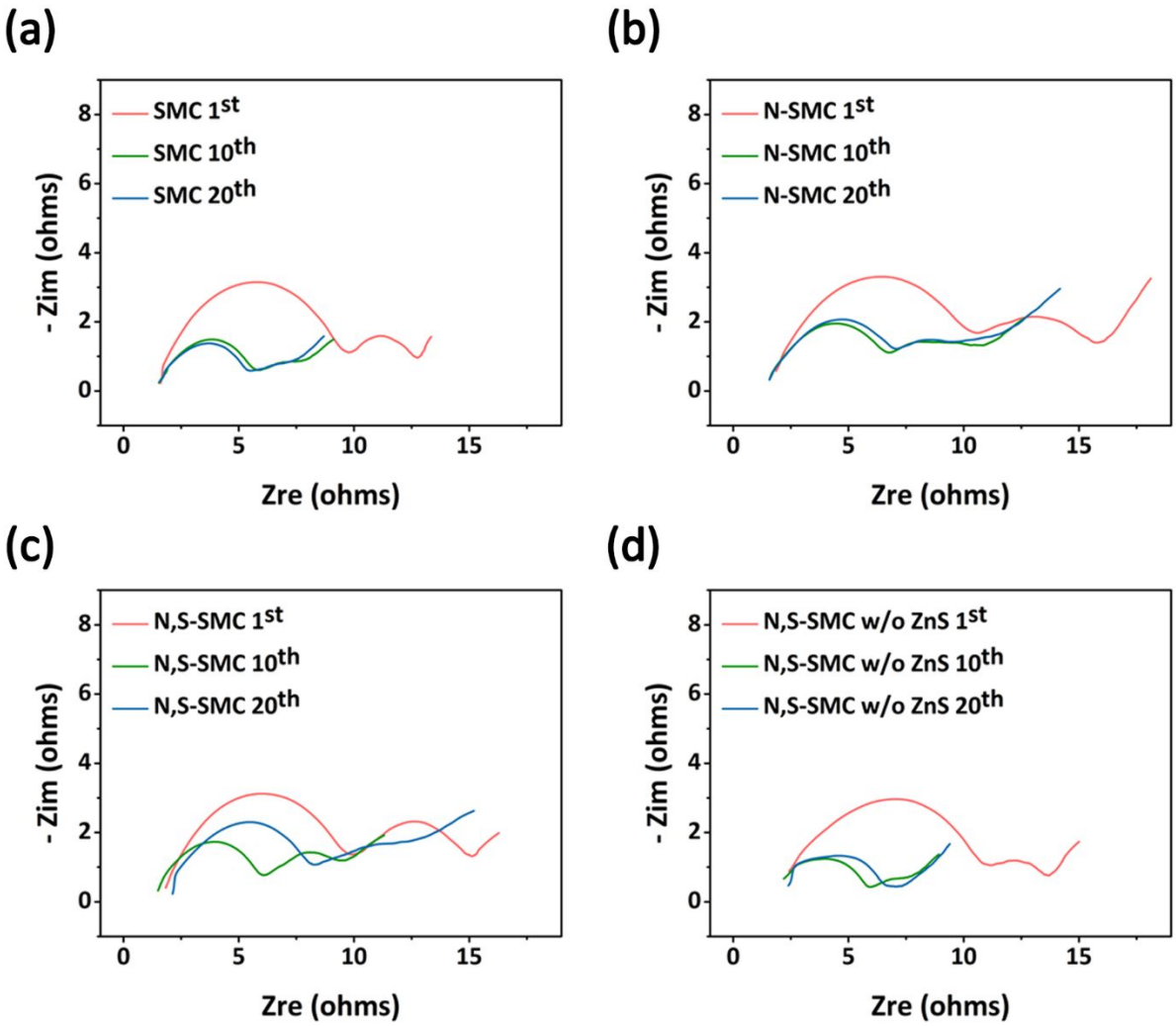

Figure S13. Electrochemical impedance spectroscopy (EIS) results of (a) SMC, (b) N-SMC, (c) N,S-SMC, and (d) N,S-SMC w/o ZnS for Li-S batteries at 1st, 10th, and 20th cycles.

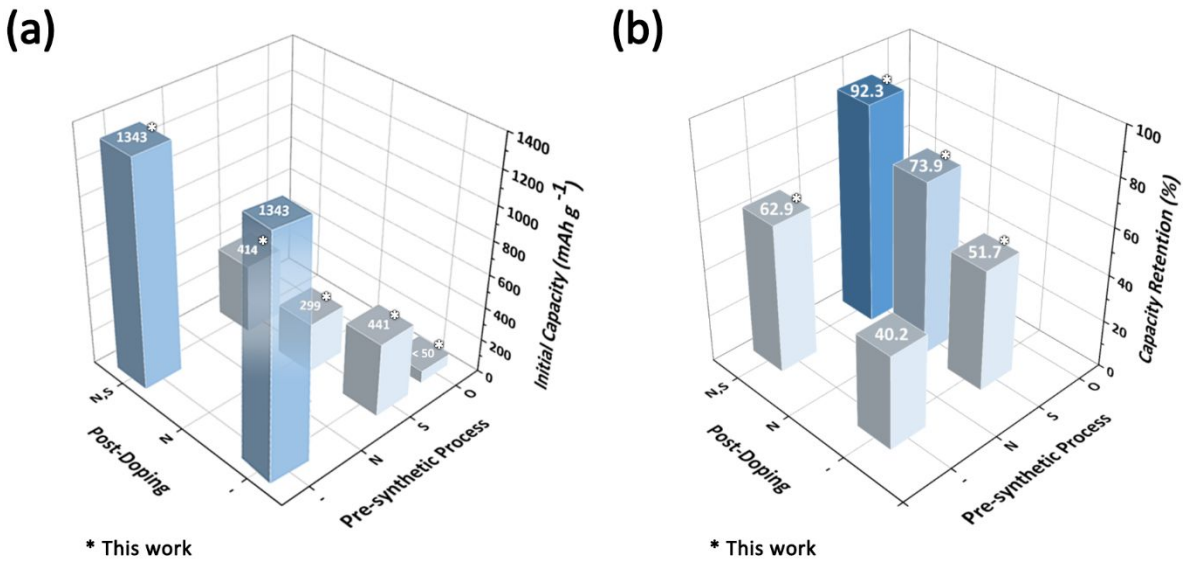

Figure S14. 3D histograms of (a) initial capacity and (b) capacity retention of pre-synthetic processed and post-doped MOF derived porous carbon employed as cathodes for Li-S battery.

Pre-doping Source (Doped Atom)	Post-doping Source (Doped Atom)	Sample	Binder	Conductive Additives	Electrolyte	Ref.
$BDC\text{-}(SH)_2$ (S)	-	SMC	SBR/CMC	Super P	1 M LiTFSi in DOL/DME (1:1 v/v) with 0.1 M $LiNO_3$	This work
	Melamine (N)	N-SMC				
	Thiourea (N,S)	N,S-SMC				
BDC (-)	-	HPCN	PVDF*	Acetylene black	1 M LiTFSi in DOL/DME (1:1 v/v)	[38]
	-	MWCNT@Meso-C	PVDF*	Super P	1.5 M LiTFSi in DOL/DME (1:1 v/v)	[39]
	Thiourea (N,S)	NSMC	SBR/CMC	Ketjenblack	1 M LiTFSi in DOL/DME (1:1 v/v) with 0.1 M $LiNO_3$	This work

* PVDF: Polyvinylidene fluoride

Table S1. Detailed experimental conditions of Li-S batteries in **Table 3**.

Limiting Current Density ($mA \cdot cm^{-2}$)		Pre-synthetic Process			
		-	N	S	O
Post-doping	-	-2.7[33]	-3.3[36]	-3.92	-4.9[37]
	N	-3.2[33]	-	-4.21	-5.85[37]
	N,S	-3.0[33]	-	-5.19	-

Table S2. Limiting current density of pre-synthetic processed and post-doped MOF derived porous carbons employed as catalysts for oxygen reduction reaction.

Half-wave Potential (V vs RHE)		Pre-synthetic Process			
		-	N	S	O
Post-doping	-	0.76[33]	0.8[36]	0.787	0.81[37]
	N	0.76[33]	-	0.805	0.902[37]
	N,S	0.83[33]	-	0.81	-

Table S3. Half-wave potential of pre-synthetic processed and post-doped MOF derived porous carbons employed as catalysts for oxygen reduction reaction.

Initial Capacity ($mAh \cdot g^{-1}$)		Pre-synthetic Process			
		-	N	S	O
Post-doping	-	1177[38] or 1343[39]	466	441	< 50
	N	-	-	299	-
	N,S	1343	-	414	-

Table S4. Initial capacity of pre-synthetic processed and post-doped MOF derived porous carbons employed as cathodes for Li-S battery.

Capacity Retention (%)		Pre-synthetic Process			
		-	N	S	O
Post-doping	-	64.6[38] or 40.2[39]	42.6	51.7	-
	N	-	-	73.9	-
	N,S	62.9	-	92.3	-

Table S5. Capacity retention of pre-synthetic processed and post-doped MOF derived porous carbons employed as cathodes for Li-S battery.

Pre-synthetic Source (Doped Atom[a])	Post-doping Source (Doped Atom[a])	Sample	Sulfur Loading	C-rate[b]	Initial Capacity ($mAh \cdot g^{-1}$)	Capacity Retention (% ($mAh \cdot g^{-1}$))	Cycle Number	Ref.
$BDC\text{-}(SH)_2$ (S)	-	SMC	70 wt%	0.1 C	441	21.7% (228) 44.8% (197)	50 100	This work
	Melamine (N)	N-SMC	70 wt%	0.1 C	299	73.9% (221) 65.5% (196)	50 100	
	Thiourea (N,S)	N,S-SMC	70 wt%	0.1 C	414	92.3% (382) 85.2% (353)	50 100	
			60 wt%	0.1 C	701	41.2% (289)	50	

***** Detailed experimental conditions such as types of binder, conductive additives, and electrolyte vary from sample to sample, which can be found in **Table S1**.

[a] We noted additional doped atoms compared to the reference which uses Zn as a metal ion, BDC as an organic ligand, and no additional post-doping.

[b] 1 C = 1675 $mA \cdot g^{-1}$

Table S6. Summary of SMC, N-SMC, N,S-SMC with 70 wt% sulfur loading and N,S-SMC with 60 wt% sulfur loading as cathodes for Li-S battery.